Dalton Transactions

Diversity and uniformity in anion-π complexes of thiocyanate with the aromatic, olefinic and quinoidal π-acceptors.

Journal:	*Dalton Transactions*
Manuscript ID	DT-ART-05-2020-001654.R1
Article Type:	Paper
Date Submitted by the Author:	22-May-2020
Complete List of Authors:	Wilson, Joshua; Ball State University Maxson, Tristan; Ball State University Wright, Isabelle; Ball State University Zeller, Matthias; Purdue University Rosokha, Sergiy; Ball State University

SCHOLARONE™
Manuscripts

Please do not adjust margins

ARTICLE

Diversity and uniformity in anion-π complexes of thiocyanate with the aromatic, olefinic and quinoidal π-acceptors.

Received 00th January 20xx,
Accepted 00th January 20xx

DOI: 10.1039/x0xx00000x

Joshua Wilson,[a] Tristan Maxson,[a] Isabelle Wright,[a] Matthias Zeller,[b] and Sergiy V. Rosokha*[a]

Despite the progress in the study of anion-π interactions, there are still inconsistencies in the use of this term and the experimental data about factors affecting the strength of such bonding are limited. To shed light on these issues, we explored supramolecular associations between NCS^- anions and a series of aromatic, olefinic or quinoidal π-acceptors. Combined experimental and computational study revealed that all these complexes were formed by an attraction of the anion to the face of the π-system, and the arrangements of thiocyanate followed the areas of the most positive potentials on the surfaces of the π-acceptors. The stabilities of the complexes increased with the π-acceptor strength (reflected by their reduction potentials), and were essentially independent of the magnitudes of the maximum electrostatic potentials on their surfaces. The complexes showed intense absorption bands in the UV-Vis range, and the energies of these bands were correlated with the difference of the redox potentials of the anions and π-acceptors. Such features, as well as results of Atoms-in-Molecules and Non-Covalent Indices analyses suggested that besides electrostatics, molecular orbital interactions play a substantial role in the formation of these complexes. The unified trends in variations of the characteristics of the complexes between thiocyanate and a variety of π-acceptors point to their common nature. To embrace diversity and uniformity of the anion-π associates, we suggest (following the halogen bond's definition) that anion-π bonding occurs when there is evidence of a net attraction between the anions and the face of the electrophilic π-system.

Introduction

The study of the counter-intuitive anion-π bonding advanced during the last two decades from the question "do they exist?" to the applications of this supramolecular interaction for molecular recognition, anion transport, catalysis, etc.[1-5] Early examples of the association between π-acceptors (also referred to as π-acidic systems) and halide anions which currently might be classified as anion-π complexes were observed in solutions by Briegleb and Davis more than 50 years ago.[6] In the 1980s, complexes between halides and hexafluorobenzene were characterized by Hiraoka in the gas phase.[7] During the 1990s, attractive interaction between negative charges and polarizable aryls were observed in host-guests systems by Schneider,[8] and "π-facial" interactions between Cl^- anions and the $[S_4N_3]^+$ ring was reported in the solid state by Woollins.[9] Yet a surge of interest into anion-π bonding started only in the early 2000s, when a few theoretical papers demonstrated the viability of this counter-intuitive interaction,[1] and an attraction between anions and electron-deficient π-systems was validated experimentally.[10-13] In the following years, anion-π interactions became one of the most explored phenomena among the newly-recognized supramolecular interactions (such as halogen, chalcogen or pnikogen bondings).[14-16] Most work in this area was focused on the analysis of X-ray structures showing short contacts between anion and π-systems in the solid state and/or computational investigations of anion-π bonding.[1-3,14-16] Formation of solution-phase complexes was observed mostly in the systems in which anion-π interaction was reinforced by the electrostatic attraction between the anions and cationic π-acceptors, or by hydrogen bonding.[17,18] Another approach relied on the design of polydentate host molecules capable of forming multiple bonds between π-acceptor cites and single anions.[19,20] This led to variation in the anion-π binding strength depending on the fit of the anion size to the hosts' cavities (which allowed separation or selective transport of the anions). Such complexes also showed correlation between the association energies and the values of maximum potential on the surface of the aromatic rings.[15,16] Surprisingly, the experimental data about the effects of electronic properties of π-acceptors on anion-π bonding involving single neutral π-systems are very limited.[20-22] Several previous studies of solution-phase complexes resulting from such solitary bonding were focused on the association of halide anions with p-benzoquinones, tetracyanopyrazine or hexaazatriphenylene-hexacarbonitrile.[11,23,24] In contrast to the monoatomic halides, interactions of polyatomic anions with π-systems led to a variety of donor/acceptor arrangements (reported in a number of X-ray structural and computational studies of such complexes).[15, 25-27] Solution-phase measurements of the thermodynamics of such interaction are scarce.

[a] Department of Chemistry, Ball State University, Muncie, Indiana, 47306, United States. E-mail: svrosokha@
[b] Department of Chemistry, Purdue University, West Lafayette, Indiana, 47907, United States

† Electronic Supplementary Information (ESI) available: details of UV-Vis studies, crystallographic analysis and computations. See DOI: 10.1039/x0xx00000x

Please do not adjust margins

Another surprising aspect regarding the literature on anion-π bonding is the variation in the meaning of this term itself. In many contributions, it is defined as an attraction between a negatively charged species and an electron-deficient aromatic ring, or more narrowly as "an electrostatic attraction between an anion positioned over the centroid of an aromatic ring".[2,28,29] Besides aromatics, there are other important electron π-acceptors that form complexes with anionic species, e.g. olefinic (e.g. tetracyanoethylene) and quinoidal derivatives.[11,24,30] A more broad definition of anion-π bonding as "noncovalent interactions between anions and electron-deficient π-systems"[31] take into account such molecules. Still, the comparison of similarities or distinctions in interactions of anions with different types of π-systems is lacking.

In the current work, we present the results of the combined experimental and computational analysis of complex formation between thiocyanate anions, NCS^-, with a variety of common organic π-acceptors illustrated in Chart 1. The rod-like NCS^- anion represents an ambidentate ligand which can form strong coordination compounds as well as supramolecular complexes with various electrophiles.[32] Several solid-state anion-π associates involving thiocyanate had been characterized using X-ray structural analysis.[25,33] The complexes resulted from the cooperative binding of NCS^- with two electron-deficient aromatic rings (so it is nested in the cavity of the macrocyclic host) were characterized in solutions using fluorescence titrations.[34] Thus, thiocyanates appear to be a suitable probe (beyond the simplest monoatomic halides) for a study of anion-π bonding with a single neutral π-system. The series of π-acceptors in Chart 1 includes aromatic, heteroaromatic and olefinic molecules as well as benzoquinone derivatives. These diverse π-acceptors allow to examine similarities and differences in the interactions of anions with a variety of π-systems and to elucidate factors determining the properties of such complexes.

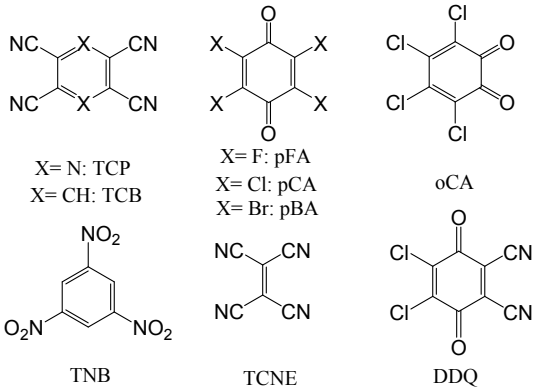

Chart 1. Structures and acronyms of the π-acceptors**.**

Results and discussion

Solution-phase association of thiocyanate with π-acceptors.

Addition of $[Bu_4N][NCS]$, salt to a solution of a π-acceptor from Chart 1 resulted in an immediate appearance of new absorption bands in the 350 – 550 nm range. An example of the spectral changes resulting from an increase of the concentration of NCS^- in the acetonitrile solution with a constant concentration of TCNE is illustrated in Figure 1. Interaction of thiocyanate with the other π-acceptors from Chart 1 in acetonitrile or dichloromethane produced similar UV-Vis spectral changes (Figures S1 – S5 in the ESI). Variable-temperature studies showed that the intensities of the new bands increases with decrease of the temperature of the solutions at constant concentration of reactants (Figure S6 in the ESI).‡ Job's plots (dependencies of the band intensities on the ratio of concentrations of donors and acceptors in the solutions with constant sum of the concentrations of reactants) show a maximum at the 1:1 ratio of reactants (Figure S7 in the ESI).

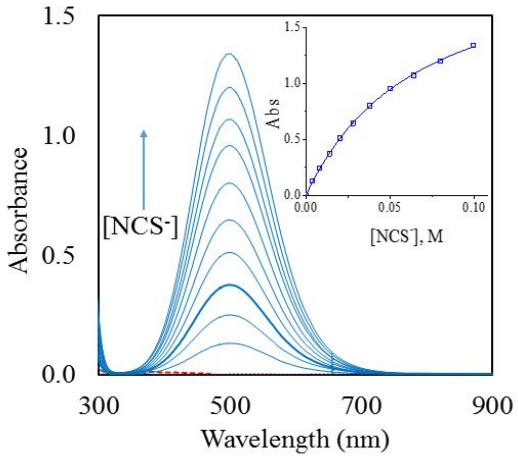

Figure 1. Spectra of solutions with constant concentration of TCNE and variable concentration of $[Bu_4N][NCS]$, (in CH_3CN, at 22 °C). Insert: The fit of absorption intensity at λ=500 nm using 1:1 TCNE/NCS^- binding model.

The variations of the bands' intensities as a function of the concentrations of NCS^- anions (at constant concentrations of acceptors) were well-modelled using a 1:1 binding isotherm.§ All these data are consistent with the predominant formation of 1:1 complexes of π-acceptors (A) and NCS^-:

$$A + NCS^- \overset{K}{\rightleftarrows} [A,NCS^-] \qquad (1)$$

The fit of the absorption data (Figure 1 and Figures S1 – S5 in the ESI) allowed to establish formation constants of the [A, NCS^-] complexes, K, as well as their extinction coefficients (Table 1).

Table 1. Spectral characteristics and formation constants of the anion-π [A,NCS^-] complexes.[a]

	E_{red},[a]	Acetonitrile		Dichloromethane	
A	V vs SCE	λ (log ε)	K^b, M^{-1}	λ (log ε)	K^b, M^{-1}
TCB	-0.65	415(3.0)	0.4±0.1	428(2.8)	2.7±0.5
TNB	-0.42	386(3.7)	0.2±0.1	396(3.3)	0.4±0.1
TCP	-0.20	461(3.4)	2.8±0.4	476(3.4)	85±15
pFA	-0.01	471(3.7)	3.6±0.5	472(3.6)	11±2
pBA	0.02			485[c]	
oCA	0.15			475[c]	
TCNE	0.17	500(3.8)	15±2	506(3.8)	147±15
DDQ	0.52			513[c]	

a) Reduction potentials, ref. 35. b) Determined at variable ionic strength.§ c) At -90 °C (Figure S8 in the ESI). Measurements of K and ε at r.t. were hindered by side-reactions.

This journal is © The Royal Society of Chemistry 20xx

The data in Table 1 indicate that the formation constants of the complexes in dichloromethane were higher than those in more polar acetonitrile. Also, the absorption band maxima of the complexes in CH_2Cl_2 are red-shifted as compared to the complexes in acetonitrile. These data also revealed two trends in the variation of spectral and thermodynamic characteristics of associates of NCS^- with various acceptors. First, the formation constants of the complexes generally rise with the shift of the reduction potentials of π-acceptors, E_{red}, to more positive values (i.e, the K values for complexes with TCNE were the highest, and those with TCB and TNB were the lowest). Second, all these complexes are characterized by intense absorption bands in the UV-Vis with ε values in the 10^3 - 10^4 M^{-1} cm^{-1} range. The absorption band maxima are shifted to longer wavelengths with increase of the E_{red} values of the π-acceptors. In fact, the absorption bands' energies of the [A,NCS^-] complexes follow the same Mulliken correlation[36] as the reported earlier anion-π associates with halide anions (Figure 2).[24]

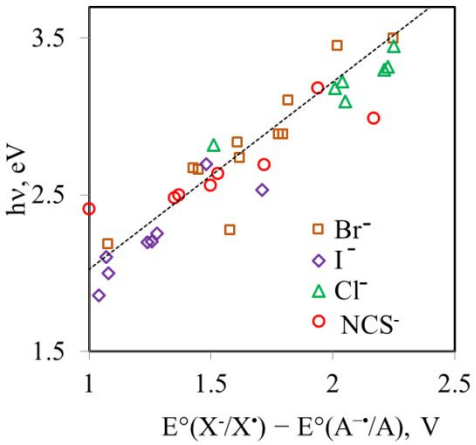

Figure 2. Correlation between the energies of absorption bands of complexes of π-acceptors A with halide or NCS^- anions, X^- (as indicated) and differences of the redox potentials (see Table S1 in ESI for details).

These unified trends suggest a similar nature of all these complexes. To compare their structural features, we first established the structures of their solid-state associates using X-ray crystallography.

2. X-ray structural analysis of solid-state associates of thiocyanate with π-acceptors.

Co-crystallization of $[Pr_4N][NCS]$ salt with the acceptors from Chart 1 produced three types of anion-π bonded associations. In particular, diffusion of hexane into dichloromethane solutions containing $[Pr_4N][NCS]$ and TCNE or TCP produced co-crystals comprising discrete 2:1 (NCS^-/A) complexes (Figure 3) surrounded by the Pr_4N^+

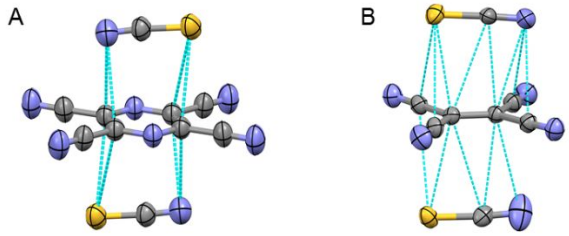

Figure 3. X-ray structures of 2:1 complexes of NCS^- with TCP (A) or TCNE (B). Contacts shorter than the sum of the van der Waals radii are shown as blue lines.

counter-ions (Figure S9 in the ESI). The anions are located on both sides of the π-acceptors, and they were essentially parallel to their planes. In complexes with TCP, the anions are arranged over the middle of the aromatic rings, perpendicular to the N-N axes.¶ The distances between the terminal atoms of thiocyanate and the carbon atoms of the TCP ring are slightly shorter than the sum of their van der Waals radii (Table 2). The terminal N and S atoms of NCS^- are slightly tilted in the general direction of the TCP plane (with N-C-S angles being about 175°), which suggests that the interaction between π-system and thiocyanate occurs mostly via the anions' terminal atoms.

Table 2. Characteristics of the solid state associations.

A	NCS^-:A[a]	Short contacts[b]	$d_{X\cdots C}$, Å	R[b]
TCP	2:1	N···C	3.150 (15)	0.97
		S···C	3.377(7)	0.97
TCNE	2:1	C···C	3.063(9)	0.90
		S···C	3.191(3)	0.91
TNB	2:2	C···C	3.141(5)	0.92
		S···C	3.296(4)	0.94
FA	2:3	N···C	2.997(3)	0.92
		S···C	3.133(2)	0.90

a) Stoichiometry of the associations. b)) The shortest contact of this type is listed. c) $R = d_{X\cdots C}/(r_X + r_C)$ where r_X and r_C are van der Waals radii (from ref. 37).

In complexes with TCNE, the disordered NCS^- anions were arranged atop the central double bonds of the π-acceptor. The S···C distance of 3.191 Å and the C···C distance of 3.067 Å were about 10 % shorter than the van der Waals separations of these atoms (Table 2).

Evaporation of the acetonitrile solution containing equimolar mixtures of trinitrobenzene and $[Pr_4N][NCS]$ resulted in formation of co-crystals with a 1:1 (NCS/TNB) ratio. They comprise wire-like 1D-stacks of alternating TNB and NCS^- moieties (a similar motif was observed previously in a number of solid-state structures of various anions and π-acceptors[25,38]). The NCS^- anions are nested between the planes of two trinitrobenzenes, and in turn, opposite sides of each TNB molecule show short contacts with two NCS anions (Figure S10 in the ESI). Each NCS anion is located over the edge of the aromatic rings of both its TNB neighbors, with the NCS axis essentially parallel to the aromatic C-C bond (Figure 4).

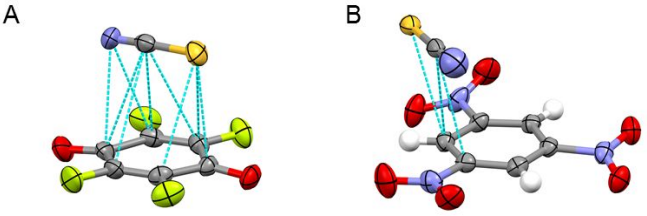

Figure 4. Fragments of the X-ray structures of co-crystals of $[Pr_4N][NCS]$ with TNB (A) and pFA (B) showing anion-π bonding of thiocyanate with the (closest) π-acceptors.

Co-crystals formed from $[Pr_4N][NCS]$ and fluoranil showed a 2:3 (NCS^-/pFA) stoichiometry. They comprise quazi-2D donor/acceptor layers separated by counter-ions. Each π-acceptor is bonded to two NCS^- anions, which are located in the cavities formed by three

acceptor moieties (Figure S10 in the ESI). The NCS^- anions are placed noticeably closer to one of their neighbors than to the other two acceptor moieties forming the cavity. Within these (closest) NCS^-/pFA pairs, thiocyanates are located almost parallel to the O-O axis (Figure 4A), with distances between carbonyl carbons and N and S atoms of thiocyanates of 2.996 Å and 3.133 Å, respectively.

Overall, X-ray analysis revealed diverse structural features of the co-crystals formed by thiocyanate and π-acceptors with various stoichiometry and distinct donor/acceptor arrangements of their anion-π associates. To check if such arrangements were the results of anion-π interactions (and not just crystal packing forces), and to find the factors determining structural features and thermodynamics of anion-π complexes, we turned to computational studies.

3. Computational analysis of the complexes.

The geometries of the BQ·X^- associates were fully optimized via M062X/def2tzvpp calculations using the Gaussian 09 suite of programs (see Experimental and the ESI for details).[39,40] To facilitate comparison with the results of UV-Vis measurements in solutions, the following discussion will focus on the data obtained via computations using the PCM model with acetonitrile or dichloromethane as the medium.[41] Previous works showed that moderately-polar solvents (e.g., dichloromethane) are the optimal medium for modelling solid-state intermolecular interactions involving ionic compounds.[42,43]

Geometry optimizations produced several minima for each A•NCS^- pair (see Figures S11 and S12 in the ESI). The lowest-energy structures (Figure 5) reproduced very well donor/acceptor arrangements obtained from the X-ray structural analysis (even though the solid-state associates were formed via 2:1, 2:2 or 2:3 donor/acceptor interactions).

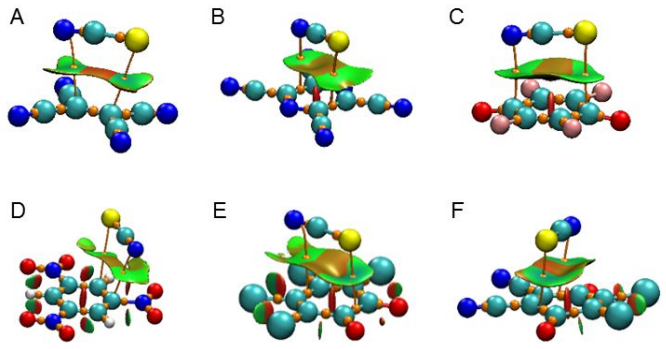

Figure 5. Superposition of the results of Atoms-in-Molecules(AIM) and Non-Covalent Indices (NCI) analyses onto the structures of complexes of NCS^- with TCNE (A), TCP (B), TNB (C) , pFA (D) oCA(E) and DDQ (F). The bond paths and critical (3, -1) points (from AIM) are shown as orange lines and spheres, respectively, and blue-green areas indicate bonding interactions (from NCI).

In the optimized dyads, thiocyanate anions were arranged atop the faces of π-molecules, with the axes of anions essentially parallel to the planes of the acceptors. Similar to the experimental structures in Figures 3 and 4, NCS^- rods were arranged over the middle of the ring in the complex with TCP, atop the C=C bond in the TCNE•NCS^- dyad, parallel to the O-O axis in complexes with p-benzoquinones and over the periphery of the aromatic ring in the TNB•NCS^- complex. The interatomic distances in the calculated complexes (Table 3) were somewhat shorter than those in the experimental X-ray structures. These distinctions are probably related to the differences between 1:1 bonding in the calculated complexes versus the 2:1, 2:2 or 2:3 interactions in solid-state associates (calculations of the 2:1 NCS^-/TCNE triads produced complexes in which N···C and N···S separations were within experimental errors of that in the X-ray structures, see Figure S13 in the ESI).

Table 3. Calculated characteristics of the [A,NCS] complexes.[a]

A	ΔE,[b] kcal/mol	$d_{N\cdots C}$,[c] Å	$d_{S\cdots C}$, Å	λ, nm (log ε)	Δq,[d] e
TCB	-5.8	3.144	3.529	458 (2.9)	0.060
TNB	-5.6	3.015[e]	3.247	394 (3.7)	0.070
TCP	-8.9	2.990	3.364	483 (3.4)	0.076
pCA	-9.1	2.832	3.123	432 (3.8)	0.161
pFA	-9.1	3.839	3.091	418 (3.8)	0.155
pBA	-9.2	2.841	3.132	435 (3.8)	0.164
oCA	-10.7	3.130	2.992	423 (4.0)	0.214
TCNE	-10.8	2.833	3.019	448 (4.0)	0.223
DDQ	-14.2	2.788	3.004	446 (3.9)	0.265

a) From calculations with CH_2Cl_2 as a medium, see Table S3 in the ESI for the data in CH_3CN. b) $\Delta E = E_c - (E_{BQ} + E_X) + BSSE$, where E_c, E_{BQ} and E_X are sums of the electronic and ZPE of the optimized complex, BQ and anion and BSSE is a basis set superposition error, see Table S4 in the ESI for details. c) Shortest intermolecular N···C distance, if not noted otherwise. d) From AIM analysis. e) N···N distance.

The interaction energies in the calculated complexes are listed in Table 3 and in Table S3 in the ESI. The variations in the ΔE values in complexes with different π-acceptors generally follow the trend in the changes of formation constants in Table 1. In accordance with the higher formation constants of [A, NCS^-] complexes in dichloromethane, the values of ΔE calculated in this medium are, on average, about 1.4 kcal/mol more negative than those calculated in acetonitrile. Spectral characteristics of the complexes obtained from the TD DFT calculations are also reasonably close to the corresponding experimental values (e.g. mean absolute deviations between the calculated and experimental values of energies and logε of absorption bands in dichloromethane are 0.23 eV and 0.18, respectively).

Overall, the consistency of the experimental and calculated structural, thermodynamic and spectral characteristics of the anion-π complexes verified that the principal structural features of the solid-state associates are not distorted by crystal forces. This also showed that computations produced accurate models of the complexes and allowed us to take a closer look at the bonding between NCS^- anions and π-acceptors.

Atoms in Molecules (AIM) analysis[44] of the optimized complexes revealed the presence of (3,-1) critical points (CP) located between terminal atoms of thiocyanate and either carbon atoms (with p-benzoquinones, TNB or TCNE) or midpoints C-C bonds in the ring (with TCP, TCB and oCA) of π-acceptors (Figure 5 and Figure S14 in the ESI). Characteristics of these points are similar to those found in many hydrogen or halogen bonded complexes.[44,45] Specifically, the values of the electron density ρ were in the 0.008 to 0.018 a.u. range, the Laplacians of the electron density, $\nabla^2\rho$ were in a 0.024 to 0.048 a.u. range and the total energy densities, H(r), were in a

This journal is © The Royal Society of Chemistry 20xx

0.0005 to 0.0016 a.u. range (Table S5 in the ESI). The AIM analysis also revealed the presence of (3, +1) or (3, +3) CPs between the central carbon atoms of the thiocyanates and the π-molecules. In particular, the complexes of NCS^- with TCNE and TNB, in which anions are located essentially over carbon-carbon bonds show (3,+1) ("ring") CPs between central (carbon) atom of thiocyanate and the center of carbon-carbon bond of the π-acceptor (Figure S14B and F in the ESI). The complexes of thiocyanate with TCP, oCA, DDQ and pFA, in which anions are located over the ring, show (3, +3) ("cage") CPs between the middle of NCS^- and the center of the π-acceptor's ring (Figure S14in the ESI). The "ring" and "cage" CPs indicate points for which one curvature in electron density changes is negative and two positive and which are minima found in cavities surrounded by multiple rings, respectively. In contrast to the (3, -1) CPs, which are located on the bond path, "ring" and "cage" CPs are "surrounded" by bond paths.[44] This suggests that formation of anion-π complexes results mostly from the attraction of the terminal (N and S) atoms of thiocyanate to the π-acceptors. This suggestion was confirmed by the Non-Covalent Indices (NCI) analyses (which determines whether an interaction is bonding or repulsive based on the deviations of the reduced gradient of density in the system from that for a homogenous electron gas).[46] It showed blue-green areas (corresponding to the negative values of sign(λ_2)) between terminal atoms of NCS^- and π-acceptors indicating attractive interactions (Figure 5 and Figure S15 in the ESI).[§§] It also demonstrated brown-reddish areas between central carbon atoms and acceptor moieties (around the locations of "ring" and "cage" CPs). Such coloring corresponds to the positive values of sign(λ_2), indicating a repulsive interaction.[46] The AIM treatment also showed very substantial charge transfer from the NCS^- anion to the π-acceptor moiety, Δq (Table 3, note that the Δq values obtained from the Natural Bond Orbital analysis[47] were close to those from AIM, see Table S5 in the ESI). The variations of Δq values generally followed changes in the interaction energies.

To establish factors determining structural and thermodynamic features of the anion-π complexes, we first compared donor/acceptor arrangements and interaction energies with the areas of the most positive potentials on the surfaces of the π-acceptors (π-holes) and the magnitude of the maximum values of these potentials (Figure 6, see values of V_{max}^{π} in Figure S17 in the ESI).

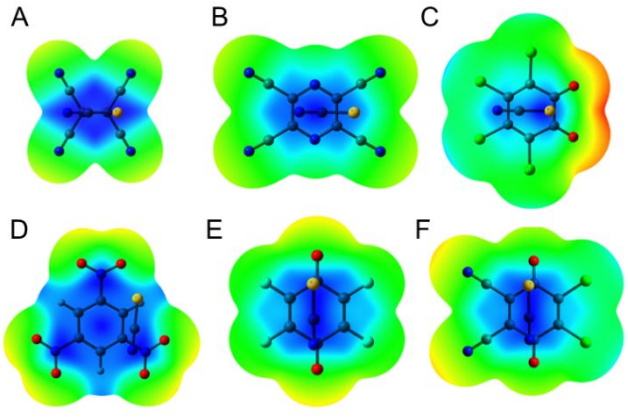

Figure 6. Superposition of the structures of A•NCS^- dyads onto the ESP surfaces of the individual acceptors: TCNE (A), TCP(B), TNB (C), pFA (D), oCA (E) and DDQ(F).

The superposition of the optimized structure of the complexes on the ESP surfaces of the corresponding π-acceptor showed that locations of NCS^- anions closely matched the area of the most positive potentials (Figure 6). This indicates that electrostatics play a primary role in anion-π complex formation, and that the ESP surfaces represent a good guide for predicting the arrangements of the NCS^- anions. However, the strength of the anion-π interactions in these complexes were not related to the magnitudes of the maximum potential, V_{max} (the correlation between ΔE and V_{max}^{π} is characterized by $R^2 \sim 0.01$, Figure 7).

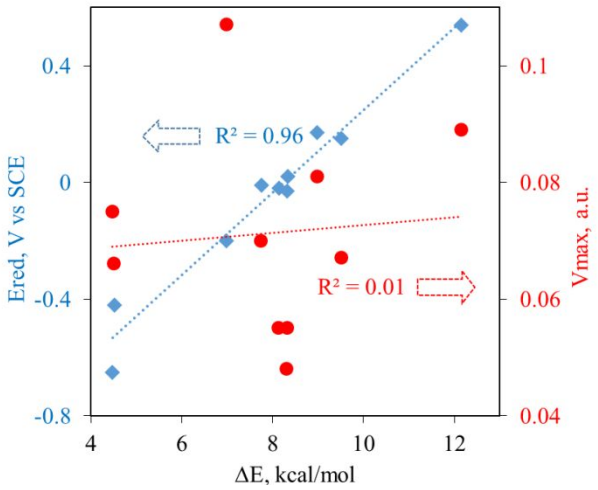

Figure 7. Relations between the ΔE values for A·NCS^- dyads and the reduction potentials of the π-acceptors, E_{red} (♦), or maximum electrostatic potential on their surface, V_{max} (●).

The ΔE values were however well correlated with the reduction potentials of the π-acceptors (R^2 = 0.96). A similar correlation between ΔE and E_{red} was observed earlier in complexes of halide anions with p-benzoquinones.[24] This indicates that the strength of the anion-π interaction is related to the overall electron-acceptor strength (as reflected by its reduction potentials).

The absence of a correlation between V_{max} and ΔE could be related to the fact that the ESP surfaces of π-acceptors and NCS^- anions (which determine the strength of electrostatic interaction) are substantially altered in the complexes by mutual polarization[48] (it was shown that polarization has a large contribution to the binding).[21a] Also, the strength of the electrostatic donor/acceptor interaction in the A•NCS^- dyads is associated with the integral attraction between NCS^- rods and the extended faces of π-acceptors. Such attraction is quite different from the point-charge interaction energies relevant for the construction of the ESP surfaces (or more localized attractions of nucleophiles to the σ-holes in halogen or hydrogen bonding). However, a comparison of the ESP surfaces in Figure 6 with the results of the AIM and NCI analysis in Figure 5 revealed another surprising feature about the relationship between electrostatics and bonding in the A•NCS^- dyads. Specifically, NCS anions are characterized by negative potentials over all their surfaces (Figure S18 in the ESI) and the most positive potential of the TCP molecule is located over the center of its aromatic ring (Figure S17 in the ESI). Thus, one might expect a strong electrostatic attraction between this area and the NCS^- anion located over the ring. However, the NCI analysis indicated repulsion between the center of the ring and the carbon

atom of NCS^-. Similar repulsive interactions of π-acceptors with the middle sections of NCS^- anions are observed in all other complexes. Moreover, while AIM analysis showed (3,-1) critical points between each terminal atom of NCS^- and π-acceptors, it also produced "ring" or "cage" CPs between the middle section of thiocyanate and the π-acceptors (Figure S14 in the ESI). This suggests that thiocyanate is bonded to the π-acceptors via its terminal atoms. Noticeably, the major segments of HOMO of NCS^- donors are located on these atoms, and their symmetries are well suited for the bonding interactions with the LUMOs of the π-acceptors (Figure 8).

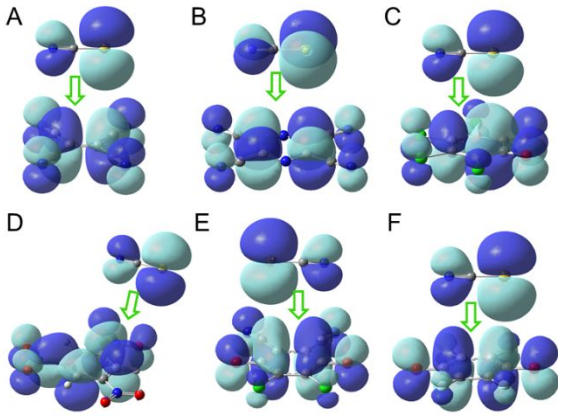

Figure 8. Illustration of formation of A•NCS^- complexes via interactions of the HOMO of NCS^- and the LUMOs of TCNE (A), TCP(B), TNB (C), pFA (D), oCA (E), DDQ(F).

Thus, while the analysis of the contributions of the various components to the interaction energies in the anion-π complexes is beyond the scope of the current work, the results of the AIM and NCI analyses, as well as the presence of the intense absorption bands in the UV-Vis spectra of the complexes[49] suggest that alongside electrostatics, molecular-orbital (HOMO/LUMO) interactions play a vital role in their formation.

Comment: Anion-π bonding - what's in the name. Experimental and computational data presented herein demonstrate common trends in variations of the characteristics of the diverse A•NCS^- associates. Notably, the NCS^- anions are located over the center of aromatic rings or their periphery, and some of these complexes are formed by olefinic or quinoidal π-acceptors. The only shared structural feature of all complexes is the location of anions atop the faces of π-systems. It indicates that limitation of anion-π complexes to those in which the anion located over aromatics or the center of the ring is too restrictive. Also, anion-π interactions are frequently defined as the attractions of the anions to the π-holes on the surfaces of molecules.[14-16] While this definition provides a sound description of many such associates, there are some issues in its applications. First, there is a question of whether π-holes may in some cases be better described as σ-holes.[50] Second, whereas thiocyanates are arranged over the area of maximum potentials on the surfaces of the acceptors in the A•NCS^- associates, the locations of the anions in many other complexes deviate substantially from the π-hole locations.[51] For example, the TCP acceptor shows a π-hole over the center of its ring. Yet, we demonstrated earlier that halides are located over its periphery (which facilitate HOMO/LUMO interactions) regardless of the anion, counter-ion, or stoichiometry of complex.[51] Actually, many publications suggest that besides (or instead) of electrostatic attraction to the π-hole, anion-π bonding is related primarily to the attraction of anions to the dipole moments of substituents[52] or weakly-covalent (charge-transfer) interactions.[24, 53] Indeed, there might be arguments in favor (or against) one or another component of anion-π bonding and the importance of contributions of these components probably varies in different systems. Similar arguments about the nature and components of interaction energies are common for the other supramolecular interactions, e.g. halogen or hydrogen bonding.[45,54] However, although there were earlier questions about the relationship between the complexes of nucleophilic and electrophilic halogens,[55] the definition of halogen bonding as an attraction between electrophilic regions of halogen atoms and a nucleophile[56] provided a rigorous framework for the discussions of its nature. Similarly, it appears that *anion-π bonding occurs when there is evidence of a net attraction between the face of an electrophilic π-system and anions*. This broad definition in terms of interacting species (consistent with that by Frontera et al.)[31] encompasses the diverse yet uniform supramolecular associates reported previously and in the current work and it circumvents the debatable question of the driving forces of anion-π bonding. Overall, consensus about the definition would facilitate the discussion of the nature and, in general, further studies of this fascinating phenomenon.

Experimental

Materials and methods. $[Bu_4N][NCS]$ salt and π-acceptors were purified by recrystallization or sublimation. $[Pr_4N][NCS]$ was prepared as described earlier.[55] CH_2Cl_2 and CH_3CN (HPLC grade) were freshly distilled over P_2O_5 under dry argon before use.

UV-Vis measurements were performed under Ar atmosphere. Formation constants and extinction coefficients of anion-π complexes were evaluated via UV-Vis titrations (see the ESI for the details). To avoid complications from the possible followed-up reactions, the room-temperature spectra were measured under argon atmosphere immediately after mixing.

Crystallography. Crystals of pFA·$[Pr_4N][NCS]$, TCNE·2($[Pr_4N][NCS]$), and TCP·2($[Pr_4N][NCS]$) were prepared by diffusion of hexane into dichloromethane solutions containing π-acceptors and $[Pr_4N][NCS]$ salt at -75 °C. TNB·$[Pr_4N][NCS]$, crystals were prepared by the evaporation of a solution of a 1:1 mixture of acceptor and salt in acetonitrile at 0 °C, under reduced pressure. Crystallographic, data collection and structure refinement details are presented in Table S4 in the ESI. Complete crystallographic data, in CIF format, have been deposited with the Cambridge Crystallographic Data Centre. CCDC 1984456-1984459 contain the supplementary crystallographic data for this paper. These data can be obtained free of charge via www.ccdc.cam.ac.uk/data_request/cif

Computations. Geometries of the complexes and reactants were optimized without constraints via DFT calculations with the M06-2X functional and def2tzvpp basis set using the Gaussian 09 suite of programs.[42,43] Calculations with wB97XD[57] produced similar results and trends (see the ESI). Calculations in acetonitrile and dichloromethane were carried out using the polarizable continuum model.[44] Values of ΔE were determined as: $\Delta E = E_c - (E_{BQ} + E_X) +$ BSSE, where E_c, E_{BQ} and E_X are sums of the electronic energies and the ZPE of the optimized complex, BQ and anion, and BSSE is a basis

This journal is © The Royal Society of Chemistry 20xx

set superposition error.[58] Since the formation of the complexes involves the deformation of BQ, these values can be expressed as $\Delta E = \Delta E_{strain} + \Delta E_{bind}$, where ΔE_{bind} is a binding energy between deformed reactants. The ΔE_{bind} values are listed in Table S in the ESI. They follow the same trends as those of ΔE. UV-Vis spectra were obtained via TD-DFT calculations, and the degree of charge transfer was estimated via AIM and NBO calculations using geometries of the complexes optimized in acetonitrile. AIM and NCI analyses were performed and visualized using Multiwfn and VMD programs, respectively.[59,60] Characteristics of the complexes are listed in the ESI.

Conclusions

Experimental and computational studies of association between thiocyanate and a series of π-acceptors demonstrated that all of them resulted from the attraction between anions and the face of the π-systems. The locations of the thiocyanates followed closely the areas of the most positive potentials on the surfaces of the π-acceptors, and the stabilities of these complexes were increasing with the π-acceptor strength (as reflected by the increase of their reduction potentials). The results of AIM and NCI analyses, as well as spectral features of the complexes suggested that besides electrostatics, molecular-orbital (charge-transfer) interactions are important factors in their formation. Overall, these results indicate a uniformity of the anion-π complexes regardless of the nature of the π-acceptor and the location of the anion over its face, and provides a guide for predicting structural features and variations of strength of these associates.

Conflicts of interest

There are no conflicts to declare

Acknowledgements

We thank the National Science Foundation for the financial support of this work (grant CHE-1607746). X-ray structural measurements were supported by the National Science Foundation through the Major Research Instrumentation Program under Grant No. CHE 1625543 (funding for the single crystal X-ray diffractometer).

Notes and references

‡ Variable-temperature measurements produced enthalpy of complex formation of -2.6 kcal/mol and -1.3 kcal/mol for complexes of thiocyanate with pFA and TCP, respectively.

§ Similarly to the reported previously formation constants of the anion-π complexes involving neutral π-acceptors,[11,19b,20d,23] the K values in this work were measured without added electrolyte, i.e. under conditions of the variable ionic strengths (the available data show that while ionic strength affects strongly complex formation between two charged species, its effect on the association of ions and neutral molecules is minor).[61] Note, that in systems with the high values of K (e.g. TCNE/NCS^-) at high concentration of NCS^-, the variation of absorption intensity deviated from the 1:1 binding model and the maximum of absorption band shifted. In agreement with X-ray structural data (vide infra), these results indicated formation 2:1 NCS^-/A complexes. As such, values of ε and K in such systems were determined in the concentration ranges where such effects were negligible.

¶ The reported co-crystals of TCP and TNB with $[Bu_4N][NCS]$, comprised infinite alternating 1D-stacks in which anions were nested between the planes of the (tilted) neighboring acceptor moieties.[25] The mutual arrangements of the anions and π-acceptors in the stacks were similar to that in co-crystals with the Pr_4N^+ counter-ions and in the calculated dyads. In particular, NCS^- were arranged over the middle of the aromatic ring in the systems with TCP, and NCS^- were located over the periphery of the rings in associations of TNB. Besides, all associations showed multiple intermolecular contacts shorter than van der Waals separations regardless of the counter-ion. There were some distinctions, however, in the co-crystals with different counter-ions. For example, while earlier co-crystallization of TCP with $[Bu_4N][NCS]$, resulted in formation of 1D-stacks, the use of Pr_4N^+ counter-ions afforded isolated 2:1 complexes. In the 2:1 complexes, the axes of the NCS^- anions were located over middle of the C-C bond, while in the 1D-stacks, the NCS^- axes deviate toward one of the carbons (probably due to crystal forces resulting from the non-parallel arrangements of the tilted TCP neighbors). Overall, the available data indicate that while the replacement of the counter-ion may result in the change of the stoichiometry of the co-crystals and minor variations of the structures, the main features of the anion-π complexes of thiocyanate are retained in the co-crystals with the different counter-ions.

§§The NCI index is the reduced gradient of the density s which describes deviation of the system from a homogenous electron gas. An isosurface of s determines the spatial areas of the interaction, and the signs of the 2nd eigenvalue of the density Hessian determines whether the interaction is bonding ($\lambda_2 < 0$) or repulsive ($\lambda_2 > 0$).[46]

1 (a) D. Quinonero, C. Garau, C. Rotger, A. Frontera, P. Ballester, A. Costa and P. M. Deya, *Angew. Chem. Int. Ed.*, 2002, **41**, 3389–3392; (b) I. Alkorta, I. Rozas and J. Elguero, *J. Am. Chem. Soc.*, 2002, **124**, 8593–8598; (c) M. Mascal, A. Armstrong and M. D. Bartberger, *J. Am. Chem. Soc.*, 2002, **124**, 6274–6276.
2 (a) A. Frontera, P. Gamez, M. Mascal, T. J. Mooibroek and J. Reedijk, *Angew. Chem. Int. Ed.*, 2011, **50**, 9564-9583; (b) B. L. Schottel, H. T. Chifotides and K. R. Dunbar, *Chem. Soc. Rev.*, 2008, **37**, 68–83.
3 P. Gamez, T. J. Mooibroek, S. J. Teat, H. T. Chifotides and K. R. Dunbar, *Acc. Chem. Res*., 2013, **46**, 894-906.
4 (a) Y. Zhao, Y. Cotelle, L. Liu, J. López-Andarias, A. B. Bornhof, M. Akamatsu, N. Sakai and S. Matile, *Acc. Chem. Res.*, 2018, **51**, 2255–2263; (b) Y. Zhao, Y. Cotelle, N. Sakai and S. Matile, *J. Am. Chem. Soc.*, 2016, **138**, 4270–4277.
5 (a) A. Vargas Jentzsch, D. Emery, J. Mareda, P. Metrangolo, G. Resnati and S. Matile, *Angew. Chem. Int. Ed.*, 2011, **50**, 11675–11678; (b) J. Mareda and S. Matile, *Chem. Eur. J.*, 2009, **15**, 28–37.
6 (a) G. Briegleb, W. Liptay and R. Fick, *Z. Elektrochem.*, 1962, **66**, 859–862; (b) K. M. C. Davis, *J. Chem. Soc. B*, 1969, **8**, 1020-1022.
7 (a) K. Hiraoka, S. Mizuse and S. Yamabe, *J. Phys. Chem.*, 1987, **91**, 5294 – 5297; (b) K. Hiraoka, S. Mizuse and S. Yamabe, *J. Chem. Phys.*, 1987, **86**, 4102-5.
8 H. J. Schneider, F. Werner and T. Blatter, *J. Phys. Org. Chem.*, 1993, **6**, 590-4.
9 J. R. Galan-Mascaros, A. M. Z. Slawin, J. D. Woollins and D. J. Williams, *Polyhedron*, 1996, **15**, 4603–4605.

10 S. Demeshko, S. Dechert and F Meyer, *J. Am. Chem. Soc.*, 2004, **126***,* 4508–4509.
11 Y. S. Rosokha, S. V. Lindeman, S. V. Rosokha and J. K. Kochi, *Angew. Chem., Int. Ed.*, 2004, **43**, 4650-4652.
12 O. B. Berryman, V. S. Bryantsev, D. P. Stay, D. W. Johnson and B. P. Hay, *J. Am. Chem. Soc.*, 2007, **129**, 48–58.
13 J. Reedijk, *Acc. Chem. Res.*, 2007, **40**, 435–444.
14 A. Bauzá, T. J. Mooibroek and A. Frontera, *Chem. Phys. Chem.*, 2015, **16**, 2496–2517.
15 (a) M. Giese, M. Albrecht and K. Rissanen, *Chem. Rev.*, 2015, **115**, 8867–8895. (b) M. Savastano, C. García-Gallarín, M. D. López de la Torre, C. Bazzicalupi, A. Bianchi and M. Melguizo, *Coord. Chem. Rev.*, 2019, **397**, 112–137.
16 H. Wang, W. Wang and W. J. Jin, *Chem. Rev.*, 2016, **116 (9)**, 5072–5104.
17 (a) M. Müller, M. Albrecht, J. Sackmann, A. Hoffmann, F. Dierkes, A. Valkonen and K. Rissanen, *Dalton Trans.*, 2010, **39**, 11329–11334; (b) M. Giese, M. Albrecht, T. Repenko, J. Sackmann, A. Valkonen and K. Rissanen, *Eur. J. Org. Chem.*, 2014, **2014**, 2435–2442. (c) M. Savastano, C. Bazzicalupi, C. Giorgi, C. García-Gallarín, M. D. López de la Torre, F. Pichierri, A. Bianchi and M. Melguizo, *Inorg. Chem.*, 2016, **55**, 8013–8024.
18 (a) M. Giese, M. Albrecht, T. Krappitz, M. Peters, V. Gossen, G. Raabe, A. Valkonen and K. Rissanen, *Chem. Commun.*, 2012, **48**, 9983–9985; (b) O. B. Berryman, F. Hof, M. J. Hynes and D. W. Johnson, *Chem. Commun.*, 2006, 506–508; (c) O. B. Berryman, A. C. Sather, B. P. Hay, J. S. Meisner and D. W. Johnson, *J. Am. Chem. Soc.*, 2008, **130**, 10895–10897.
19 (a) L. Adriaenssens, C. Estarellas, A. V. Jentzsch, M. Martinez Belmonte, S. Matile and P. Ballester, *J. Am. Chem. Soc.*, 2013, **135 (22)**, 8324–8330; (b) D.-X. Wang and M.-X. Wang, *J. Am. Chem. Soc.*, 2013, **135**, 892–897; (c) X. Lucas, A. Bauzá, A. Frontera, and D. Quinonero, *Chem. Sci.*, 2016, **7**, 1038–1050; (d) H. Zeng, P. Liu, G. Feng and F. Huang, *J. Am. Chem. Soc.*, 2019, **141**, 16501–16511.
20 (a) D.-X. Wang, Q.-Y. Zheng, Q.-Q. Wang and M.-X. Wang, *Angew. Chem. Int. Ed.*, 2008, **47**, 7485–7488; (b) L. Leoni, R. Puttreddy, O. Jurček, A. Mele, I. Giannicchi, F. Y. Mihan, K. Rissanen and A. Dalla Cort, *Chem. Eur. J.*, 2016, **22**, 18714–18717; (c) D.-H. Tuo, Y.-F. Ao, Q.-Q. Wang and D.-X. Wang, *Org. Lett.*, 2019, **21**, 7158–7162; (d) L. Adriaenssens, G. Gil-Ramírez, A. Frontera, D. Quiñonero, E. C. Escudero-Adán and P. Ballester, *J. Am. Chem. Soc.*, 2014, **136**, 3208–3218; (e) J. Xi and X. Xu, *Phys. Chem. Chem. Phys.*, 2016, **18**, 6913–6924. (f) M.-D. Gu, Y. Lu and M.-X. Wang, *J. Org. Chem.*, 2020, **85**, 2312–2320.
21 (a) P. Ballester, *Acc. Chem. Res.*, 2013, **46**, 874–884. (b) M. Giese, M. Albrecht and K. Rissanen, *Chem. Commun.*, 2016, **52**, 1778–1795.
22 (a) G. Gil-Ramírez, E. C. Escudero-Adán, J. Benet-Buchholz and P. Ballester, *Angew. Chem. Int. Ed.*, 2008, **47**, 4114–18. (b) C. S. Anstöter, J. P. Rogers and J. R. R. Verlet, *J. Am. Chem. Soc.*, 2019, **141**, 6132–6135.
23 H. T. Chifotides, B. L. Schottel, K. R. Dunbar, *Angew. Chem. Int. Ed.* **2010**, *49*, 7202–7207.
24 S. Kepler, M. Zeller and S. V. Rosokha, *J. Am. Chem. Soc.*, 2019, **141**, 9338–9348.
25 B. Han, J. J. Lu and J. K. Kochi, *Cryst. Grow. Des.*, 2008, **8**, 1327-1334.
26 M. Giese, M. Albrecht, G. Ivanova, A. Valkonen and K. Rissanen, *Supramol. Chem.*, 2012, **24**, 48-55.
27 (a) A. Bauzá, T.J. Mooibroek and A. Frontera, *Cryst. Eng. Comm.*, 2016, **18***,* 10-23; (b) C. Estarellas, D. Quiñonero, P. M. Deyà and A. Frontera, *Chem. Phys. Chem.*, 2013, **14**, 145–154.
28 B. P. Hay and R. Custelcean, *Cryst. Grow. Des.*, 2009, **9**, 2539–2545.
29 M. M. Watt, M. S. Collins and D. W. Johnson, *Acc. Chem. Res.*, 2013, **46**, 955–966.
30 K. Molčanov, G. Mali, J. Grdadolnik, J. Stare, V. Stilinović and B. Kojić-Prodić, *Cryst. Grow. Des.*, 2018, **18**, 5182–5193.
31 (a) S. Brooker, N. G. White, A. Bauzá, P. M. Deyà and A. Frontera, *Inorg. Chem.*, 2012, **51**, 10334–10340; (b) M. Müller, M. Albrecht, V. Gossen, T. Peters, A. Hoffmann, G. Raabe, A. Valkonen and K. Rissanen, *Chem. Eur. J.*, 2010, **16**, 12446–12453.
32 (a) P. Cauliez, V. Polo, T. Roisnel, R. Llusar and M. Fourmigué, *Cryst. Eng. Comm.*, 2010, **12**, 558–566; (b) J. Viger-Gravel, I. Korobkov and D. L. Bryce, *Cryst. Grow. Des.*, 2011, **11**, 4984–4995; (c) S. V. Rosokha, C. L. Stern, A. Swartz and R. Stewart, *Phys. Chem. Chem. Phys.*, 2014, **16**, 12968–12979
33 M. Savastano, C. García, M. D. López de la Torre, F. Pichierri, C. Bazzicalupi, A. Bianchi and M. Melguizo, *Inorg. Chim. Acta.*, 2018, **470**, 133–138.
34 H.-B. Liu, Q. Zhang and M.-X. Wang, *Angew. Chem. Int. Ed.*, 2018, **57**, 6536–6540.
35 (a) S. V. Rosokha and J. K. Kochi, *Acc. Chem. Res.*, 2008, **41**, 641-653; (b) M. T. Huynh, C. W. Anson, A. C. Cavell, S. S. Stahl and S. Hammes-Schiffer, *J. Am. Chem. Soc.*, 2016, **138**, 15903–15910.
36 R. S. Mulliken and W. B. Person, Wiley: New York, 1969.
37 A. Bondi, *J. Phys. Chem.*, 1964, **68**, 441–451.
38 S. V. Rosokha and A. Kumar, *J. Molec. Struct.*, 2017, **1138**, 129-135.
39 Gaussian 09, Revision C.01, M. J. Frisch, G. W. Trucks, H. B. Schlegel, G. E. Scuseria, M. A. Robb, J. R. Cheeseman, G. Scalmani, V. Barone, B. Mennucci, G. A. Petersson, H. Nakatsuji, M. Caricato, X. Li, H. P. Hratchian, A. F. Izmaylov, J. Bloino, G. Zheng, J. L. Sonnenberg, M. Hada, M. Ehara, K. Toyota, R. Fukuda, J. Hasegawa, M. Ishida, T. Nakajima, Y. Honda, O. Kitao, H. Nakai, T. Vreven, J. A. Montgomery, Jr., J. E. Peralta, F. Ogliaro, M. Bearpark, J. J. Heyd, E. Brothers, K. N. Kudin, V. N. Staroverov, R. Kobayashi, J. Normand, K. Raghavachari, A. Rendell, J. C. Burant, S. S. Iyengar, J. Tomasi, M. Cossi, N. Rega, J. M. Millam, M. Klene, J. E. Knox, J. B. Cross, V. Bakken, C. Adamo, J. Jaramillo, R. Gomperts, R. E. Stratmann, O. Yazyev, A. J. Austin, R. Cammi, C. Pomelli, J. W. Ochterski, R. L. Martin, K. Morokuma, V. G. Zakrzewski, G. A. Voth, P. Salvador, J. J. Dannenberg, S. Dapprich, A. D. Daniels, O. Farkas, J. B. Foresman, J. V. Ortiz, J. Cioslowski and D. J. Fox, Gaussian, Inc., Wallingford CT, 2009.
40 Y. Zhao and D. G. Truhlar, *Theor. Chem. Acc.*, 2008**, 120,** 215-41.
41 J. Tomasi, B. Mennucci and R. Cammi, *Chem. Rev.*, 2005, **105**, 2999−3093.
42 K. E. Riley and K.-A. Tran, *Faraday Discuss.*, 2017, **203**, 47–60.
43 S. V. Rosokha, C. L. Stern and J. T. Ritzert, *Chem. Eur. J.*, 2013, **19**, 8774–8788.
44 (a) R. F. W. Bader, *Chem. Rev.*, 1991, ***91*** **(5)**, 893–928. (b) R.G.A. Bone, R. F.W. Bader *J. Phys. Chem.* **1996,** *100,* 10892-10911.
45 (a) S. J. Grabowski, *Chem. Rev.* 2011, **111**, 2597-2625; (b) E. Pastorczak and C. Corminboeuf, *J. Chem. Phys.*, 2017, **146**, 120901.
46 (a) E. R. Johnson, S. Keinan, P. Mori-Sánchez, J. Contreras-García, A. J. Cohen and W. Yang, *J. Am. Chem. Soc.*, 2010, **132**, 6498–6506. (b) J. Contreras-García, E. R. Johnson, S. Keinan, R. Chaudret, J.-P. Piquemal, D. N. Beratan and W. Yang, *J. Chem. Theory Comput.*, 2011, **7**, 625–632.
47 NBO Version 3.1, E. D. Glendening, A. E. Reed, J. E. Carpenter and F. Weinhold.
48 P. Politzer, J. S. Murray and T. Clark, *J. Phys. Chem. A*, 2019, **123**, 10123–10130.
49 E. V. Anslyn and D. A. Dougherty, Univ. Sci. Books, Sausalito, California, 2006, p. 186.

 This journal is © The Royal Society of Chemistry 20xx

50 S. Kozuch, *Phys. Chem. Chem. Phys.*, 2016, **18** , 30366–30369.
51 O. Grounds, M. Zeller and S. V. Rosokha, *New J. Chem.*, 2018, **42**, 10572–10583.
52 S. E. Wheeler and K. N. Houk, *J. Phys. Chem. A*, 2010, **114**, 8658–8664.
53 (a) Y. P. Yurenko, S. Bazzi, R. Marek and J. Kozelka, *Chem.-Eur. J.*, 2017, **23**, 3246–3250; (b) C. Foroutan-Nejad, Z. Badri and R. Marek, *Phys. Chem. Chem. Phys.*, 2015, **17**, 30670–30679.
54 (a) G. Cavallo, P. Metrangolo, R. Milani, T. Pilati, A. Priimagi, G. Resnati and G. Terraneo, *Chem. Rev.*, 2016, **116**, 2478–2601; (b) L. C. Gilday, S. W. Robinson, T. A. Barendt, M. J. Langton, B. R. Mullaney and P. D. Beer, *Chem. Rev.*, 2015, **115**, 7118–7195.
55 P. Metrangolo, T. Pilati and G. Resnati, *Cryst. Eng. Comm.*, 2006, **8**, 946–947.
56 G. R. Desiraju, P. S. Ho, L. Kloo, A. C. Legon, R. Marquardt, P. Metrangolo, P. Politzer, G. Resnati and K. Rissanen, *Pure and Applied Chemistry*, 2013, **85**, 1711–1713.
57 J.-D. Chai and M. Head-Gordon, *Phys. Chem. Chem. Phys.*, 2008, **10**, 6615−6620.
58 S. F. Boys and F. Bernardi, *Mol. Phys.*, 1970, **19**, 553−566.
59 T. Lu and F. Chen, *J. Comput. Chem.*, 2012, **33**, 580–592.
60 W. Humphrey, A. Dalke and K. Schulten, *J. Mol. Graphics*, 1996, **14**, 33–38.
61 (a) P. Atkins, J. de Paula, J. Keeler, *Physical Chemistry, 11th ed.* Oxford University Press., Oxford, UK, 2018, p. 797-798. (b) S. V. Rosokha, D. Sun, J. Fisher, J. K. Kochi, *ChemPhysChem, 2008, 9, 2406 – 2413.*

ToC graphic and text

Variety of anion-π complexes of thiocyanate showed common trends in changes of thermodynamic, spectral and structural features with variations in redox- and surfaces electrostatic potentials of the π-acceptor